A geometrical-based microcell mobile radio channel model

Mahmoud, Seedahmed; Hussain, Zahir; O'Shea, Peter

Mahmoud, Hussain, Z., & O'Shea, P. (2006). A geometrical-based microcell mobile radio channel model. Wireless Networks, 12(5), 653–664. https://doi.org/10.1007/s11276-006-6061-0

Published Version: https://doi.org/10.1007/s11276-006-6061-0

A Geometrical-Based Microcell Mobile Radio Channel Model

Seedahmed S. Mahmoud, Zahir M. Hussain, and Peter O'Shea

Abstract— **In this paper we present a geometric multipath propagation model for a microcell mobile environment. The proposed model provides the statistics for the direction-of-arrival (DOA) of multipath components. These statistics are required to test adaptive array algorithms for cellular applications. The proposed model assumes that 1) a line-of-sight (LOS) path exists between the transmitter and the receiver, 2) the scatterers lie within a circle of radius R around the mobile station, and 3) the base station lies within this circle. The distances between the scatterers and the mobile station are subject statistically to a hyperbolic distribution. The model also provides the multipath power delay profiles (PDP), which are used to evaluate the bit error rate (BER) and the signal to interference ratio (SIR) for the direct-sequence code division multiple access (DS-CDMA). We derive and simulate the joint probability density functions (pdfs) of the power-DOA and the power-Doppler shift. Further we determine expressions for the BER performance and for the SIR of a DS-CDMA system over the proposed channel model. A simplified expression based on the improved Gaussian approximation (SEIGA) is used to evaluate the BER and the SIR in a wideband multipath channel. Although the proposed model is applicable for downlink as well, in this paper we will analyze the uplink environment only.**

Keywords— **Channel model, DS-CDMA, microcell.**

I. Introduction

Channel modelling is an important issue for the design and analysis of mobile communication systems. A signal propagating through a wireless channel usually arrives at the destination along a number of different paths, referred to as multipaths. These paths arise from scattering, reflection, refraction or diffraction of the radiated energy off objects that lie in the environment [1]. The received signal is much weaker than the transmitted signal due to phenomena such as mean propagation loss, slow fading, and fast fading [1]. For analysing the performance of wireless communication systems, a statistical channel model (which provides information about the direction-of-arrival (DOA) and time-of-arrival (TOA) of the multipath components) is required. A common channel modelling strategy is to use a statistical description of time-variant fading effects of the physical channel due to moving terminals, moving obstacles and the transmission environment [2]. However, these types of channel models do not provide any directional information and it is not possible to derive DOAs from them. Therefore, they are not directly applicable for systems with multiple antennas [3].

Multiple access interference (MAI) is a factor which limits the capacity and performance of DS-CDMA systems. MAI refers to the interference between direct sequence users. This interference is the result of the random time offsets between signals, which make it impossible to design code waveforms to be completely orthogonal. While the MAI caused by any one user is generally small, as the number of interferers or their power increases, MAI becomes substantial. Therefore, any analysis of performance of a CDMA system has to take into account the amount of MAI and its effects on the parameters that measure the performance (most notably the signal-to-interference-and-noise ration (SINR) at the receiver and the related bit error probability on the information bit stream). Much work has been reported on the calculation of the user average BER for DS-CDMA systems. The most widely used and popular approach is the Gaussian approximation (GA) [4] and its variants.

In [5] Liberti and Rappaport devised a geometrical based single bounce model (GBSB) for microcells. The GBSB model assumes that scatterers are uniformly distributed in space and have equal scattering cross sections. Their model allows for the fact that short delay multipath components are more likely to arrive with DOA near the direct path, while multipath components with longer delays tend to be more uniformly distributed in DOA.

In [6] we proposed a space-time geometrical channel model with hyperbolically distributed scatterers for a macrocell mobile environment. This model combined a scalar stochastic fading model for the local scatterers with the geometrical hyperbolic model proposed in [7] for the distribution of the dominant scatterers. The model in [6] assumes that the scatterers are arranged circularly around the mobile, with the distances between 1) the mobile and the local scatterers and 2) the local and dominant scatterers, both being distributed hyperbolically according to an inverse-cosh-squared distribution.

In this paper, we present a statistical channel model for a microcell environment. This model is an extension of the macrocell model proposed in [7], however in this model the base station (BS) antenna is relatively low and multipath scattering near the BS is just as likely as multipath scattering near the mobile station (MS). Although in microcells environment there are two types of propagation: LOS and non-LOS propagation, In this model we will assume that there is a LOS path between the transmitter and the receiver and that the scatterers are arranged in a circle centered on the MS, with the circle radius being R. It is further assumed that the BS lies within this circle. The

S. S. Mahmoud and Z. M. Hussain are with the School of Electrical and Computer Engineering, RMIT University, Melbourne, Victoria 3000, Australia, E-mail address: s2113794@student.rmit.edu.au, zmhussain@ieee.org.

P. O'Shea is with the School of Electrical and Electronic Systems Engineering, Queensland University of Technology, Brisbane, Queensland 4000, Australia, Email: pj.oshea@qut.edu.au.

Citation:
Mahmoud, S, Hussain, Z and O'Shea, P 2006, 'A geometrical-based microcell radio channel model', Wireless Networks, vol. 12, no. 5, pp. 653-664.

distances, r_k, between the scatterers and the MS conform to a hyperbolic distribution. This assumption is more realistic and flexible than other commonly used probability density functions (pdf's), such as the uniform pdf [5]. This is so because the hyperbolic distribution allows scatterers to assume higher concentration in a flexible area in the vicinity of the mobile. For example, in an urban area the mobile would see a large number of scatterers in the immediate neighborhood, while farther buildings can also act as scatterers for waves that escaped the immediate neighborhood, but the farther we go from the mobile the fewer are the buildings that may act as scatterers, as they will be obscured by nearer buildings. Validation of this claim using practical data will be presented in Section III. The actual spread is decided by a practical parameter that depends on the specific physical environment. The proposed model assumes that each multipath component is created by a specular reflection of the propagating signal at the remote object. Once the co-ordinates of the scatterers are drawn from the reciprocal cosh distribution of r_k, all necessary channel characteristics, including direction-of-arrival, can be derived [7].

The joint pdf of the power-DOA and the power-Doppler frequency shift for the proposed channel model are derived and simulated. These pdfs are given in [8] for the macrocell channel model proposed in [7]. Further we study the performance of the DS-CDMA system over the proposed channel model. SEIGA analysis (proposed by Holtzman [4] for the case of perfect power control and extended by Liberti [9] for the case of imperfect power control) is used to evaluate the BER and SIR over the proposed microcell channel model. The multipath power delay profiles (PDP) arising from this channel for different propagation scenarios have been used as inputs to evaluate the BER and the SIR for the DS-CDMA. The performance of the system over the proposed microcell channel model has been compared with the performance over the space-time hyperbolic macrocell channel proposed in [6]. A conventional correlation receiver at the BS for both channel models has been considered. For better performance of DS-CDMA systems in this model, a general RAKE receiver will be a better option.

II. The Channel Model

In this section we introduce a geometrically-based channel model with hyperbolically distributed scatterers for a LOS microcell environment. Signals received at the BS are assumed to be plane waves arriving from the horizon and hence the DOA calculation will include only the azimuthal coordinate [1].

Fig.1 illustrates the proposed channel model. Although the model is applicable for downlink as well, we will analyze the uplink environment only. This model assumes that the scatterers are arranged within a circle of radius R around the mobile. The BS is within the scatterers' circle. The distances r_k between the mobile and the scatterers are distributed according to an inverse-cosh-squared distribution, whereas the angles of departure, ψ_k, are uniformly distributed in the interval, [0,2π]. D denotes the distance between the BS and the MS. This model is suitable for a microcell environment where $D < R$, and the BS, MS and scatterers are all in relatively close proximity. The angle θ_k is the DOA at the BS for the kth path.

The baseband complex envelope assuming omnidirectional antennas, a stationary user, and a multipath channel impulse response h_b is given by [5]:

$$h_b(t,\tau) = \sum_{k=0}^{L-1} \alpha_k \delta(t-\tau_k) = \sum_{k=0}^{L-1} \beta_k e^{j\phi_k} \delta(t-\tau_k) \qquad (1)$$

where $\beta_k = |\alpha_k|$ is the magnitude of the k$^{\text{th}}$ multipath component, ϕ_k is the phase of the multipath component, τ_k is the path delay, and L is the number of multipaths. We assume that a LOS path exists with time-of-arrival given by $\tau_0 = \frac{D}{c}$, where c is the speed of light. (1) would need to be modified if omni-directional antennas are not used at both the MS and the BS. To model the system performance with multiple antennas, it is necessary to model the DOA [5].

A. The Proposed Model Parameters

The geometrical scatter density function $f_{r_k}(r_k)$ of and ψ_k pdf are proposed to be as follows:

$$f_{r_k}(r_k) = \begin{cases} \frac{a}{\tanh(aR)\cosh^2(ar_k)} & \text{for } 0 \le r_k \le R \\ 0 & \text{elsewhere} \end{cases} \qquad (2)$$

$$f_{\psi_k}(\psi_k) = \frac{1}{2\pi} \qquad \text{where} \quad 0 \le \psi_k \le 2\pi \qquad (3)$$

where the scattering spread parameter a can assume values in the interval (0,1). A suitable value of a must be chosen for the simulation. Conveniently, formula (10) in [10] relates a to the angle spread. Thus, for a given angle spread (assumed or measured), one can use the formula in [10] to deduce an appropriate value of a. The radius of the scatterers' circle, R, controls by the scattering spread parameter a, while the distance D between the MS and the BS is chosen to be equal or within the range of the measurement distance. The cumulative probability functions for (2) and (3) are given by

$$F_{r_k}(r_k) = \begin{cases} 1 & \text{for } r_k > R \\ \frac{\tanh(ar_k)}{\tanh(aR)} & \text{for } 0 < r_k < R \\ 0 & \text{elsewhere} \end{cases} \qquad (4)$$

$$F_{\psi}(\psi_k) = \frac{\psi_k}{2\pi} \qquad \text{for } 0 \le \psi_k \le 2\pi. \qquad (5)$$

The pdf $f_{r_k}(r_k)$ in (2) for the distribution of r_k is shown in Fig. 2, where the radius of the scatterer is $R = 200$ m, and a takes the values 0.08, 0.02, and 0.06.

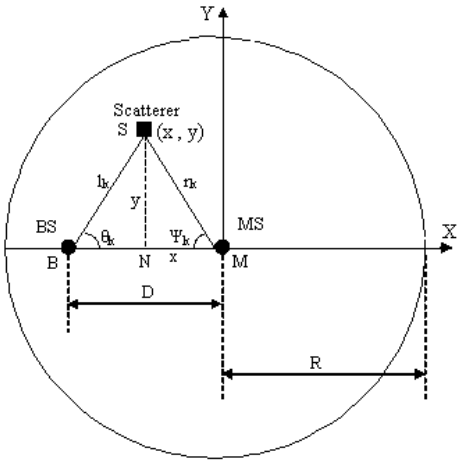

Fig. 1. Geometry of the Proposed Model. "MS" stands for the mobile station, and "BS" is the base station

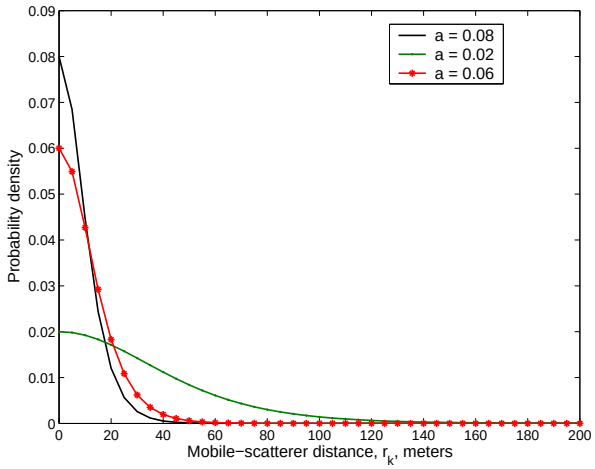

Fig. 2. The probability density, $f_{r_k}(r_k)$ for the distribution of the distance between the mobile and the k^{th} scatterer r_k: ($R = 200$ m, with $a = 0.08$, 0.02, and 0.06).

For simulation purposes, generation of samples for the random variables r_k and ψ_k can be done by using a common random number generator followed by application of some appropriate transformations. The common random number generator draws samples x_k and y_k from uniformly distributed random variables X and Y in the interval [0,1]. These samples are then transformed to create $r_k(x_k)$ and $\psi_k(y_k)$ as follows:

$$r_k = \frac{1}{a}\tanh^{-1}(x_k \tanh(a\,R)) \tag{6}$$

and

$$\psi_k = 2\pi y_k \tag{7}$$

The path delay τ_k of the k^{th} multipath component is given by

$$\tau_k = \frac{(l_k + r_k)}{c} = \frac{1}{c}\left[r_k + \sqrt{r_k^2 + D^2 - 2r_k D\cos(\psi_k)}\right] \tag{8}$$

where l_k is the distance between scatterer and the BS. Applying the law of cosine to the triangle MBS in Fig. 1 gives, $l_k = \sqrt{r_k^2 + D^2 - 2r_k D\cos(\psi_k)}$.

The DOA for the k^{th} path, θ_k, is given over $(-\pi, \pi)$ by

$$\theta_k = \begin{cases} \tan^{-1}\left(\frac{r_k\sin(\psi_k)}{D - r_k\cos(\psi_k)}\right) \\ \text{for } r_k\cos(\psi_k) \le D \ ; \\ \tan^{-1}\left(\frac{r_k\sin(\psi_k)}{D - r_k\cos(\psi_k)}\right) + \pi \\ \text{for } (r_k\cos(\psi_k) > D)\&(0 \le \psi_k \le \frac{\pi}{2}) \ ; \\ \tan^{-1}\left(\frac{r_k\sin(\psi_k)}{D - r_k\cos(\psi_k)}\right) - \pi \\ \text{for } (r_k\cos(\psi_k) > D)\&(\frac{3\pi}{2} \le \psi_k \le 2\pi) \end{cases} \tag{9}$$

The mean power of each multipath component depends on the propagation delay τ_k, and is usually defined by a characteristic power delay profile (PDP), $\mathrm{P}(\tau_k)$, which is given by [11]

$$P(\tau_k) = P_{ref} - 10\,n\,\log\left(\frac{\tau_k}{\tau_{ref}}\right) \tag{10}$$

In the above n is the path loss exponent and it depends on the propagation scenario to be simulated [11]. P_{ref} is a reference power that is measured at a distance, d_{ref}, from the transmitting antenna when omnidirectional antennas are used at both the transmitter and the receiver. The reference power is [11]

$$P_{ref} = P_T - 20\,\log\left(\frac{4\,\pi\,d_{ref}\,f_c}{c}\right) \tag{11}$$

where P_T is the transmitted power in dB and f_c is the carrier frequency. The power in each multipath component P_k is related to the magnitude α_k of the k^{th} multipath in equation (1) by

$$P(\tau_k) = P_0 + 20\log|\alpha_k|. \tag{12}$$

The above equation can be re-arranged to give

$$\alpha_k = 10^{\frac{P_k - P_0}{20}} \tag{13}$$

where P_0 is the direct path power in dB. In this paper the direct path power loss due to propagation can be defined by the Friis free space equation [11]

$$P_0(D) = P_T K\left(\frac{\lambda^2}{(4\pi)^2 D^2}\right) \tag{14}$$

where K is a constant describing the gain of the antenna and the system loss factor, and λ is the wavelength of the signal.

For the integration of this model into the simulation environment, it is necessary to limit the path delay, τ_k. The

maximum path delay $\tau_{\max}$ occurs when ψ_k =180°. From (8) we have

$$\tau_{\max} = \frac{1}{c}(D + 2r_{\max}) \tag{15}$$

where $r_{\max}$ is the distance between the mobile and the scatterer that corresponds to $\tau_{\max}$. In practice, $\tau_{\max}$ is given a value which is application dependent [5], hence, $r_{\max}$ is found as follows

$$r_{\max} = \frac{(c\tau_{\max} - D)}{2} = \frac{c(\tau_{\max} - \tau_o)}{2} = \frac{c\tau_{e\max}}{2} \tag{16}$$

where $\tau_{e\max} = \tau_{\max} - \tau_o$ is the maximum excess delay and τ_o is the direct path delay.

B. Joint Power-DOA and Power-Doppler Shift Probability Density Functions

In this subsection we derive the joint power-DOA at the MS and the power-Doppler shift pdfs for the proposed microcell channel model. Doppler spectrum accounts for the distribution of power at each DOA. It is well-known that the Doppler spectrum is dependent on the pdf of the DOA of the multipath components at the MS and the direction of motion of the mobile. The Doppler spectrum is U-shaped as noted by Clark [11], when the pdf of the DOA of the multipath components at the mobile is uniform. In this paper we consider that the transmitter is moving while scatterers are stationary (Doppler due to mobile scatterers is not considered).

The geometry utilized to derive the pdf is shown in Fig.1. It will be useful to express the joint scatterer probability density function with respect to the polar coordinates (r, ψ) as an intermediate step before deriving the joint power-DOA and the power-Doppler shift pdfs. The joint pdf $f(r, \psi\,)$ is given by

$$f(r, \psi\,) = \frac{a}{2\pi \tanh(aR) \cosh^2(a\ r)} \tag{17}$$

We apply the law of cosines to the triangle MBS in Fig.1 to derive the joint power-DOA pdf $f_{p,\psi}(p, \psi)$, where p is the power of the multipath components and ψ is the DOA at the MS. Applying this law gives

$$l^2 = D^2 + r^2 - 2\,r\,D\,\cos(\psi\,). \tag{18}$$

The total path propagation distance is given by

$$d = l + r = r + \sqrt{D^2 + r^2 - 2\,r\,D\,\cos(\psi\,)}. \tag{19}$$

Squaring both sides of (19), and solving for r as a function of d gives

$$r = \frac{D^2 - d^2}{2(D\cos(\psi) - d)}. \tag{20}$$

By applying the Jacobian transformation $J(r, \psi)$, the joint distance(d)-DOA pdf is given by

$$f_{d,\psi}(d, \psi) = \frac{D^2 + d^2 - 2Dd\cos(\psi)}{2(D\cos(\psi) - d)^2} f_{r,\psi}\big(r, \psi\big). \tag{21}$$

where $f_{r,\psi}\big(r, \psi\big)$ and r are given by (17) and (20) respectively.

The joint d-DOA pdf $f_{d,\psi}(d, \psi)$ for the proposed channel model is given by substituting (17), and (20) into (21)

$$f_{d,\psi}(d, \psi) = \frac{p(d, \psi)}{2\pi \cosh^2(g(d, \psi))} \tag{22}$$

where,

$$p(d, \psi) = \frac{a(D^2 + d^2 - 2\,D\,d\,\cos(\psi))}{2\tanh(aR)(D\cos(\psi) - d)^2} \tag{23}$$

and

$$g(d, \psi) = \frac{a\left(D^2 - d^2\right)}{2\left(D\cos(\psi) - d\right)}. \tag{24}$$

When an exponential path-loss model is assumed, the power will be related to the total path propagation distance d by [12], [11]

$$p = p_o \left(\frac{d}{D}\right)^{-n} \tag{25}$$

where p is the power level of the path related to the multipath propagation distance d, p_o is power of the direct line-of-sight path (at distance D), and n is the path loss exponent.

The above equation can be re-arranged to give

$$d = D \left(\frac{p}{p_o}\right)^{-\frac{1}{n}}. \tag{26}$$

The joint power (p)-DOA pdf $f_{p,\psi}(p, \psi)$ for the proposed channel model is given by

$$f_{p,\psi}(p, \psi) = |J(d, \psi)|\, f_{d,\psi}(d, \psi)\Big|_{d=D\left(\frac{p}{p_o}\right)^{-\frac{1}{n}}} \tag{27}$$

where the Jacobian transformation, $J(d, \psi)$, is given by

$$J(d, \psi) = \left|\ \frac{\partial d}{\partial p}\ \right| = \frac{D}{np_o \left(\frac{p}{p_o}\right)^{\frac{(n+1)}{n}}}. \tag{28}$$

Substituting (28) into (27) yields

$$f_{p,\psi}(p, \psi) = \frac{D}{np_o \left(\frac{p}{p_o}\right)^{\frac{(n+1)}{n}}} f_{d,\psi}\big(d(p), \psi\big) \tag{29}$$

The joint power-DOA pdf $f_{p,\psi}(p, \psi)$ is given by substituting (22), and (26) into (29)

$$f_{p,\psi}(p, \psi) = \ \frac{a\ D\ h(p,\psi)}{4\pi np_o \tanh(aR)\cosh^2(\Phi(p,\psi))} \tag{30}$$

where

$$h(p, \psi) = \frac{(D^2 + D^2\left(\frac{p}{p_o}\right)^{-\frac{2}{n}} - 2\,D^2\left(\frac{p}{p_o}\right)^{-\frac{1}{n}}\cos(\psi))}{\left(\frac{p}{p_o}\right)^{\frac{n+1}{n}}\left(D\cos(\psi) - D\left(\frac{p}{p_o}\right)^{-\frac{1}{n}}\right)^2} \tag{31}$$

and

$$\Phi(p,\psi) = \frac{a(D^2 - D^2\left(\frac{p}{p_o}\right)^{-\frac{2}{n}})}{2(D\cos(\psi) - D\left(\frac{p}{p_o}\right)^{-\frac{1}{n}})}. \quad (32)$$

To evaluate the joint power (p)-Doppler frequency shift (f_d) pdf, $f_{p,f_d}(p,f_d)$, we use the Doppler shift formula, which is given by [11]

$$f_d = f_m \cos(\psi - \theta_v) \quad (33)$$

where f_m is the maximum Doppler shift ($f_m = \frac{v}{\lambda}$), λ is the carrier wavelength, v is the speed of the mobile, ψ is the DOA at the mobile station, and θ_v is the direction where the mobile is travelling [11]. Solving (33) for ψ gives

$$\psi = \theta_v + \cos^{-1}\left(\frac{f_d}{f_m}\right) \quad (34)$$

The joint power-Doppler frequency pdf, $f_{p,f_d}(p,f_d)$, is given by

$$f_{p,f_d}(p,f_d) = |J(p,\psi)|\, f_{p,\psi}(p,\psi)\Big|_{\psi=\theta_v+\cos^{-1}\ \frac{f_d}{f_m}} \quad (35)$$

where $J(p,\psi)$ is the Jacobian transformation given by

$$J(p,\psi) = \left|\ \frac{\partial\psi}{\partial f_d}\ \right| = \frac{1}{f_m \sin(\psi-\theta_v)} = \frac{1}{f_m\sqrt{1-\left(\frac{f_d}{f_m}\right)^2}} \quad (36)$$

Let $\xi = \left(\frac{p}{p_o}\right)^{-\frac{1}{n}}$, then the joint power-Doppler frequency pdf, $f_{p,f_d}(p,f_d)$, is given by

$$f_{p,f_d}(p,f_d) = \sum_{i=1}^{2} \frac{a\ D\ \Upsilon_i(\xi,f_d)}{4\pi n p_o \tanh(aR)\cosh^2(\beta(\xi))} \quad (37)$$

where

$$\Upsilon_i(\xi,f_d) = \frac{(1+\xi^2-2\xi\cos(\psi_i))}{\xi^{-(n+1)}(\cos(\psi_i)-\xi)^2 f_m\sqrt{1-\left(\frac{f_d}{f_m}\right)^2}} \quad (38)$$

and

$$\beta(\xi) = \frac{aD(1-\xi^2)}{2(\cos(\psi_i)-\xi)} \quad (39)$$

where

$$\psi_i = \begin{cases} \theta_v + \cos^{-1}\left(\frac{f_d}{f_m}\right) & : i = 1 \\ \theta_v - \cos^{-1}\left(\frac{f_d}{f_m}\right) & : i = 2. \end{cases} \quad (40)$$

Fig. 3 shows the joint power-DOA pdf $f_{p,\psi}(p,\psi)$ for the proposed microcell channel model. In this simulation we considered a path loss exponent of 2 (free space), the distance between the mobile and the base station is set to D = 1 km, the scatterers' circle radius is R = 2 km, and the power of the direct LOS path, p_o, has been limited to 1 Watts. From the figure, It is evident that the powers of the other multipath components are less than the assumed direct LOS power, p_o.

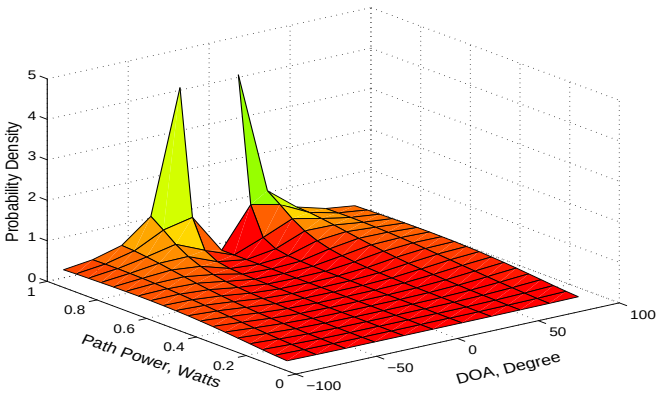

Fig. 3. The Joint power-DOA probability density function for the proposed channel model: (D = 1 km, R= 2 km, a = 0.0025, n = 2, and p_o = 1 W).

Fig. 4 shows the joint power-Doppler shift pdf $f_{p,f_d}(p,f_d)$ for the proposed microcell channel model. In this figure the direction where the mobile is travelling is set to $\theta_v = \frac{\pi}{2}$. The scatterer spread parameter a is set to 0.0033, D is set to 1 km and the scatters' circle radius is R = 1.5 km. Similarly, Fig 5 shows the joint power-Doppler frequency pdf when $\theta_v = 0$. From the simulation results we observe that the joint power-Doppler frequency pdf is highly dependent on θ_v.

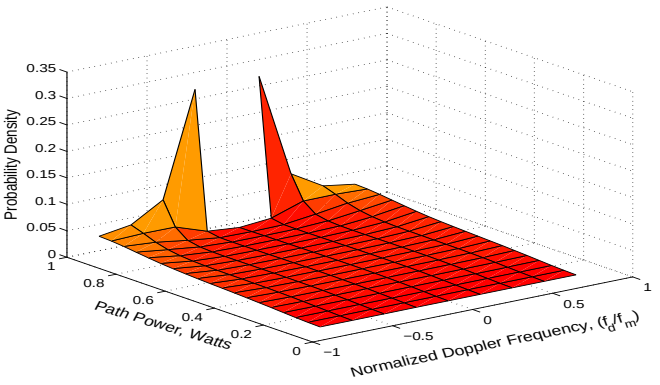

Fig. 4. The Joint power- Doppler frequency probability density function for the proposed channel model: ($\theta_v = \frac{\pi}{2}$, D = 1 km, R= 1.5 km, a = 0.0033, n = 2, and p_o = 1 W).

III. Experimental Results

In this section we verify the validity of the proposed model. The DOA at the BS pdf for this model is compared with the measurement data reported in [13] and analyzed by Janaswamy [14]. Following the Appendix we get the pdf $f(\theta)$ for the proposed model as follows:

$$f(\theta) = \int_0^{2\pi} f(\theta,\psi)\, d\psi \quad (41)$$

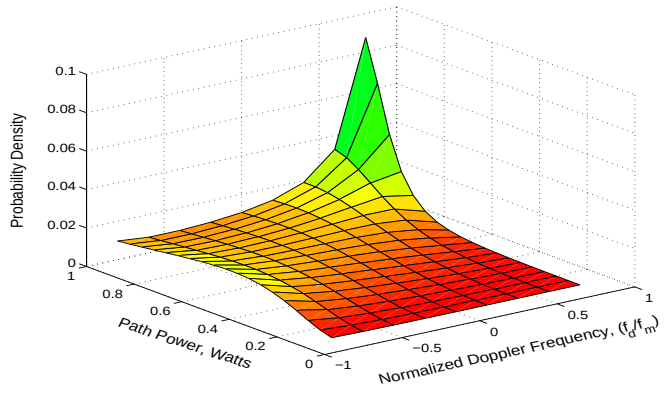

Fig. 5. The Joint power-Doppler frequency probability density function for the proposed channel model: ($\theta_v = 0$, $D = 1$ km, R= 1.5 km, $a = 0.0033$, $n = 2$, and $p_o = 1$ W).

where $f(\theta, \psi)$ is given in (63).

In [13], Spencer *et al.* conducted a number of indoor measurement results, collected at 7 GHz within office buildings on the BYU campus. The scanning was done mechanically with a 6° horn over a 360° range. At the Clyde building, the angular data measured is for data within one cluster about its mean angle. The angular spread (standard deviations) is 24.5°. Fig. 6 shows a comparison of the results for the DOA pdf for the proposed channel model versus the measurement data reported in [13]. The DOA pdf for the proposed model is evaluated numerically using eq.(41). For the proposed model, the values of D and a were determined to be 100 m and 0.028, respectively, to produce the same value of the measurement standard deviations (24.5°).

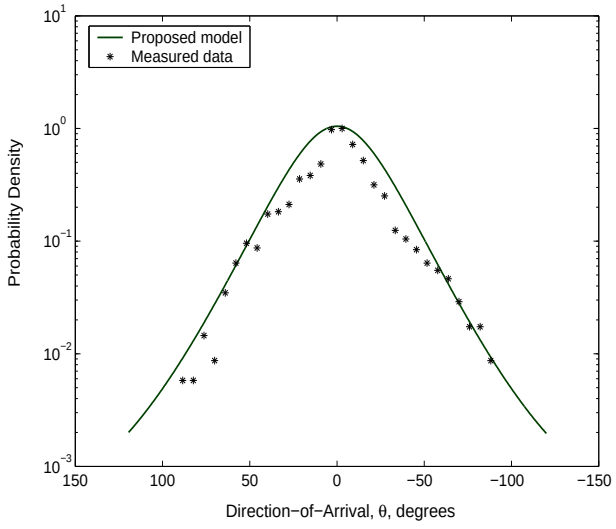

Fig. 6. A comparison of the direction-of-arrival density function for the proposed channel model with the practical measurements.

From Fig. 6, it is clear that there is a good match between the proposed channel model result and the measurement data, except for a short range of negative angles near the LOS. This is because of the measured data are asymmetric in angle implying that the scattering centers are asymmetric about the LOS direction [13], [14]. This figure shows the validity of the proposed model. Comparing with the DOA pdf for the Gaussian scatter density model (GSDM) in [14] (Fig. 10), we observe that the proposed model has a better match specially around the LOS.

IV. Performance Analysis of DS-CDMA in the Proposed Channel Model

We consider the reverse link (mobiles to base station) of a single cell asynchronous DS-CDMA system that supports M active users. This system is shown in Fig. 7.

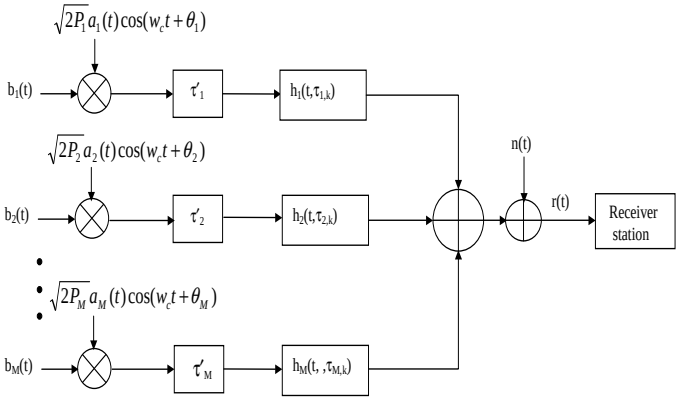

Fig. 7. A Generic DS-CDMA system model.

The m$^{\text{th}}$ transmitted signal is described by [15]

$$s_m(t-\tau_m^{'}) = \sqrt{2P_m} b_m(t-\tau_m^{'}) a_m(t-\tau_m^{'}) \cos(\omega_c t + \theta_m) \tag{42}$$

where $b_m(t)$ is the data signal, $a_m(t)$ is the spectral-spreading signal, P_m is the power of the transmitted signal, ω_c is the carrier frequency, $\tau_m^{'}$ is the time delay that accounts for the lack of synchronism between the transmitters, and θ_m is the phase angle of the m$^{\text{th}}$ carrier. The m$^{\text{th}}$ user's data signal is a sequence of unit amplitude rectangular pulses of duration T_b, taking values from {-1,+1}. with equal probability. This sequence can be expressed as

$$b_m(t) = \sum_{j=-\infty}^{\infty} b_j^m p_{T_b}(t - jT_b) \tag{43}$$

where p_{T_b}= 1, for $0 \le t < T_b$, and p_{T_b}= 0, otherwise. The spreading signal $a_m(t)$ can be expressed as

$$a_m(t) = \sum_{i=-\infty}^{\infty} a_i^m \psi(t - iT_c) \tag{44}$$

where $\psi(t)$ is a chip waveform that is time-limited to [0,T_c] and normalized to have energy T_c, where $\int_0^{T_c} \psi^2(t)dt = T_c$ is the chip period, and $a_i^{(m)}$ is the i$^{\text{th}}$ chip value of the m$^{\text{th}}$ user; this chip value can be either -1 or +1. There are N chips per bit and thus $N = \frac{T_b}{T_c}$ is the process gain for user m. We assume that the desired user is m=0 and all other users contribute to MAI.

The received signal at the input of the correlation receiver is given by

$$r(t) = \sum_{m=0}^{M-1}\sum_{k_m=0}^{L_m-1}\sqrt{2P_m}\alpha_{m,k_m}b_m(t-\tau_{m,k_m}) \times a_m(t-\tau_{m,k_m})\cos(\omega_c t+\phi_{m,k_m})+n(t) \quad (45)$$

where $n(t)$ is additive white Gaussian noise (AWGN) with a two-sided power density of $\frac{N_0}{2}$. Note that the value of θ_m is absorbed into the channel phase ϕ_{m,k_m}, while the values of $\tau_m^{'}$ is included in τ_{m,k_m}. Without loss of generality, we assume that the reference user is denoted by m=0 (user of interest). The decision statistic at the output of the correlator is given by [16], [17]

$$Z_0 = \int_0^{T_b} r(t)a_0(t-\tau_{0,0})\cos(\omega_c t)dt = b_0\,\alpha_{0,0}\sqrt{\frac{P_0}{2}}\,T_b + \sum_{m=0}^{M-1}\sum_{[k_m=0,k_0\neq 0]}^{L_m-1} I_{m,k_m} + v \quad (46)$$

where b_0 is the transmitted bit from user 0, $\alpha_{0,0}$ is the amplitude of the desired direct line-of-sight multipath component, P_0 is the transmitted power of the desired user,

$$v = \int_0^{T_b} n(t)a_0(t-\tau_{0,0})\cos(\omega_c t)dt \quad (47)$$

is a zero-mean Gaussian random variable with variance $\sigma_v^2 = \frac{N_0T_b}{4}$, and

$$I \triangleq \sum_{m=0}^{M-1}\sum_{[k_m=0,k_0\neq 0]}^{L_m-1} I_{m,k_m} = \sum_{m=0}^{M-1}\sum_{[k_m=0,k_0\neq 0]}^{L_m-1}\int_0^{T_b} G(t)dt \quad (48)$$

$(G(t) = \alpha_{m,k_m}s_m(t-\tau_{m,k_m})e^{j\phi_{m,k_m}}a_0(t-\tau_{0,0})\cos(\omega_c t))$. The formula in (48) represents the contributions of the MAI and the inter-symbol-interference (ISI) to the decision statistic. The MAI term includes: 1) all the multipath components relative to the desired user other than the line-of-sight (LOS) path ($I_{0,1}...I_{0,L_0-1}$), and 2) all the multipath components relative to the interference users: ($I_{m,0}...I_{m,L_m-1}$, $\forall\ m = 1, 2, ..., M-1$).

Thus, the decision statistic in (46) can be re-written as

$$Z_0 = D_0 + I + v \quad (49)$$

where D_0 is the desired signal component (first term in (46)), I is the MAI as given by (48), and v is the AWGN as quantified in (47).

A. SIR Performance

In wireless communications, the signal-to-interference ratio (SIR) is a predominant parameter that characterizes the system performance. In particular, SIR estimates are required for radio resource allocation tasks such as handoff, dynamic channel assignment and power control. The SIR measures the ratio between the desired user's power and the amount of interference generated by all other sources sharing the same resource. The MAI and the thermal noise components, I and v, in (49) are statistically independent. From (49), we can express the SIR as follows:

$$SIR = \frac{E\{D_0^2\}}{E\{(I+v)^2\}} = \frac{E\{D_0^2\}}{E\{I^2\}+E\{v^2\}} \quad (50)$$

The statistical averages (the useful and noise terms) in equation (50) can be given by [11]

$$E\{D_0^2\} = E\left\{\left(b_0\sqrt{\frac{P_0}{2}}\,\alpha_{0,0}T_b\right)^2\right\} = \frac{P_0T_b^2}{2}\,\alpha_{0,0}^2 \quad (51)$$

$$E\{v^2\} = \sigma_v^2 = \frac{N_0T_b}{4}. \quad (52)$$

Expression for the variance of the interference term can be found in [4], [11].

The SEIGA approach was developed in [4] to estimate the BER in DS-CDMA systems. It has been extended by Liberti [9] for the case of imperfect power control, and by Sunay and McLane [16] for the case of frequency non-selective fading channel.

The simplified SIR and BER expressions are based on the fact that if $g(x)$ is a continuous function and x is a random variable with mean value μ_x and variance σ_x^2, then the average value of this function can be expressed by making used of the Taylor's expansion [18] as follows:

$$E\{g(x)\} = g(\mu_x+x) + \frac{1}{2}\sigma_x^2 g''(\mu_x) + \ldots \quad (53)$$

The previous expression can be expanding in difference rather than derivatives [11] as given by:

$$E\{g(x)\} \approx g(\mu_x) + \frac{\sigma_x^2}{2}\frac{g(\mu_x+h)-2g(\mu_x)+g(\mu_x-h)}{h^2}. \quad (54)$$

By choosing $h = \sqrt{3}\sigma_x$, equation (54) becomes [4]

$$E\{g(x)\} \approx \frac{2}{3}g(\mu_x)+\frac{1}{6}g(\mu_x+\sqrt{3}\sigma_x)+\frac{1}{6}g(\mu_x-\sqrt{3}\sigma_x). \quad (55)$$

Using the previous expression and (50), the expression of SIR for a wideband channel model with a LOS is given by

$$SIR = E\left[\left(\frac{P_0T_b^2}{2\psi}\,\alpha_{0,0}^2\right)\right] \approx \frac{2}{3}\left(\frac{P_0|\alpha_{0,0}|^2}{\mu_\psi+\frac{N_0}{2T_b}}\right)+\frac{1}{6}\left(\frac{P_0|\alpha_{0,0}|^2}{\mu_\psi+\sqrt{3}\sigma_\psi+\frac{N_0}{2T_b}}\right) + \frac{1}{6}\left(\frac{P_0|\alpha_{0,0}|^2}{\mu_\psi-\sqrt{3}\sigma_\psi+\frac{N_0}{2T_b}}\right). \quad (56)$$

where μ_ψ and σ_ψ are the mean and standard deviation of ψ respectively, ψ is the variance of the signal-plus-interference portion of the decision statistic, and $Q(n) = \frac{1}{\sqrt{2\pi}}\int_n^\infty e^{\frac{-u^2}{2}}du$. The mean and standard deviation of ψ are [9] given by

$$\mu_\psi = \frac{1}{3N}\left(\sum_{m=1}^{M-1}\sum_{k_m=0}^{L_m-1} A_{m,k_m} + \sum_{k_0=1}^{L_0-1} A_{0,k_0}\right) \tag{57}$$

$$\begin{aligned}\sigma_\psi^2 = \frac{1}{N^4}\Bigg(&\frac{N-1}{36}\sum_{m=1}^{M-1}\sum_{l=1}^{M-1}\sum_{k=0}^{L_m-1}\sum_{j=0}^{L_m-1} A_{m,k}A_{l,j} \\ &+\frac{23N^2+8N-8}{360}\sum_{m=1}^{M-1}\sum_{k_m=0}^{L_m-1} A_{m,k_m}^2 \\ &+\frac{N-1}{9}\sum_{m=1}^{M-1}\sum_{k=0}^{L_m-1}\sum_{j=1}^{L_0-1} A_{m,k}A_{0,j} \\ &+\frac{N-1}{9}\sum_{k=1}^{L_0-1}\sum_{j=1}^{L_0-1} A_{0,k}A_{0,j} \\ &+\frac{23N^2+32N-32}{360}\sum_{k=1}^{L_0-1} A_{0,k}^2\Bigg)\end{aligned} \tag{58}$$

where $A_{m,k_m} = P_m|\alpha_{m,k_m}|^2$.

B. BER Performance

For a wideband channel model with a LOS, the SEIGA for the bit error probability is given by [9]

$$\begin{aligned}\bar{P}_e &= E\left[Q\left(\sqrt{\frac{P_0T_b^2}{2\psi}\,\alpha_{0,0}^2}\right)\right] \\ &\approx \frac{2}{3}Q\left(\sqrt{\frac{P_0|\alpha_{0,0}|^2}{\mu_\psi+\frac{N_0}{2T_b}}}\right)+\frac{1}{6}Q\left(\sqrt{\frac{P_0|\alpha_{0,0}|^2}{\mu_\psi+\sqrt{3}\sigma_\psi+\frac{N_0}{2T_b}}}\right) \\ &\quad+\frac{1}{6}Q\left(\sqrt{\frac{P_0|\alpha_{0,0}|^2}{\mu_\psi-\sqrt{3}\sigma_\psi+\frac{N_0}{2T_b}}}\right)\end{aligned} \tag{59}$$

where μ_ψ and σ_ψ^2 are given by (57) and (58) respectively.

V. Simulation Results

The proposed model has been simulated for indoor, free space, urban, and shadowed urban scenarios. We consider M users uniformly distributed at random locations throughout a circular cell. These users were located at distances in the interval (1000,1200) meters from the base station (BS) for urban, shadowed urban, and free space scenarios, and at distances in the interval (90,100) meters from the BS for indoor scenario. For each user in the cell, channels are generated using the proposed model.

For the simulations in this paper we assume that the angle spread is 13^o (for urban area, shadowed urban and free space [5]), which corresponds to $a = 0.0033$, and $R = 1.5$ km. For indoor scenario, the angle spread is assumed to be 24.5^o, which corresponds to $a = 0.028$, and $R = 200$ m. In all simulations, we set the chip rate to 8 Mb/s, the process gain N to 32, and the number of multipath components $L_k = 20$. The receiver is assumed to be omnidirectional deploying a conventional correlation type receiver. Finally, the SEIGA for the BER and SIR in (59) and (56) respectively are used to analytically determine the BER and SIR for each user.

Fig. 8 shows the envelopes for simulated multipath Rician fading using the proposed channel model with $a = 0.0033$ and two values of D (0.5 km and 0.7 km). The mobile is assumed to be moving at 74.6 mph, which corresponds to a maximum Doppler shift of 100 Hz at 900 MHz carrier. The transmitted signal is a balanced QPSK signal with a symbol rate of 9600 symbols/sec.

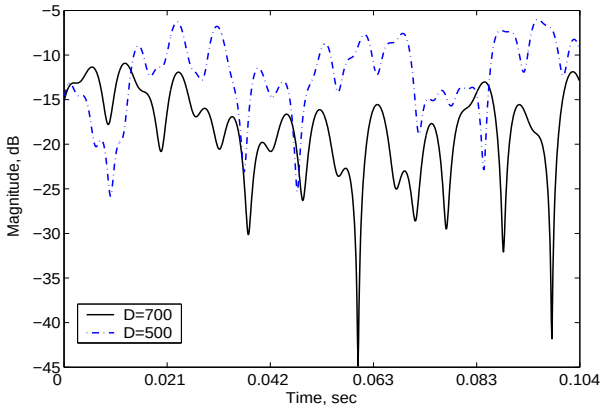

Fig. 8. Rician fading envelopes using the proposed channel model with $f_d = 100$ Hz, sampling period $T_s = 104.2\mu$s, $a = 0.0033$, and two values of D: 0.5 km and 0.7 km.

Fig. 9 and 10 show the BER and SIR performance as a function of the number of users under different propagation scenarios. The propagation scenarios are: 1) urban area with a path loss exponent of n = 3, 2) shadowed urban with a path loss exponent of n = 4, 3) free space with a path loss exponent of n = 2, and 4) indoor (LOS) scenario with a path loss exponent of n = 1.6. The number of multipath components is set to $L_k = 20$. As illustrated in Fig. 9, the system is able to support 10 users in a free space and indoor scenarios at an average BER of 10^{-5} while the system is able to support 3 and 4 users for shadowed urban and urban scenarios, respectively. It is evident that the performance of the CDMA system is different for different environments.

Fig. 11 and 12 show the BER and SIR performance comparison, respectively, between the proposed microcell channel model and the space-time hyperbolic channel model in [6] for an urban area. The number of multipath components is set to $L_m = 20$ for all users. For this simulation a conventional correlation receiver has been used for both channels. From Fig. 11, the system is able to support approximately 9 users in the proposed microcell model at an average BER of 10^{-4} while the system is able to sup-

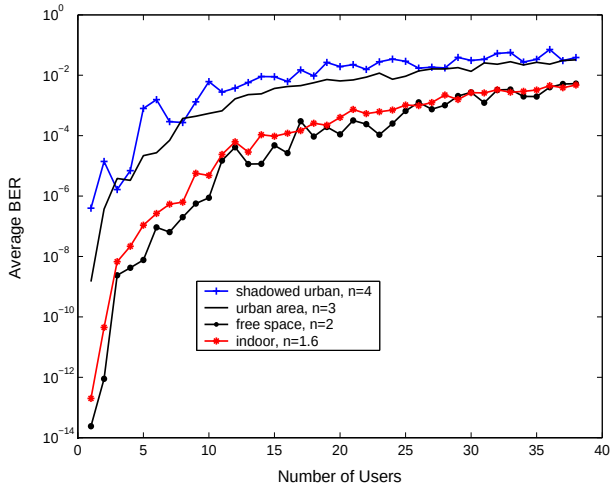

Fig. 9. BER performance as a function of the number of users under urban, shadowed urban, free space, and indoor propagation scenarios with L_k = 20, the process gain N= 32, and the chip rate = 8 Mb/s.

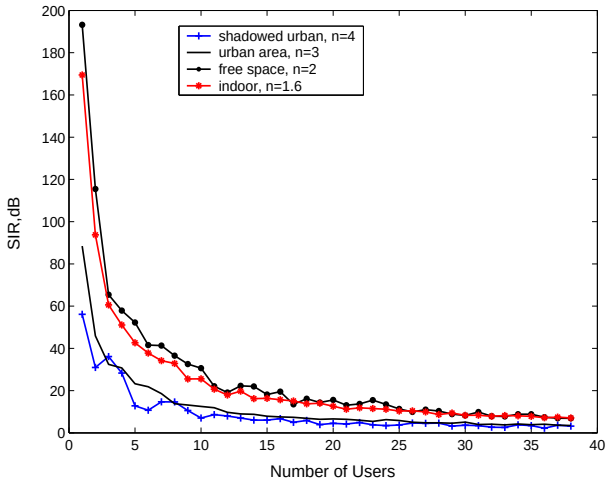

Fig. 10. SIR performance as a function of the number of users under urban, shadowed urban, free space, and indoor propagation scenarios with L_k = 20, the process gain N= 32, and the chip rate = 8 Mb/s.

port 5 users for the space-time hyperbolic macrocell channel model. This is due to the structure of the space-time hyperbolic macrocell channel, which considers local scatterers around the mobile as well as the dominant scatterers away from the mobile. The angle spread for simulating considered in simulating the space-time hyperbolic macrocell channel is assumed to be 27^o.

VI. Conclusion

A statistical geometric propagation model for a LOS microcell mobile environment is proposed. This model assumes that each multipath component is created by a specular reflection of the propagating signal at the remote object, and the distance between the scatterer and the mobile is distributed according to a reciprocal cosh-squared pdf.

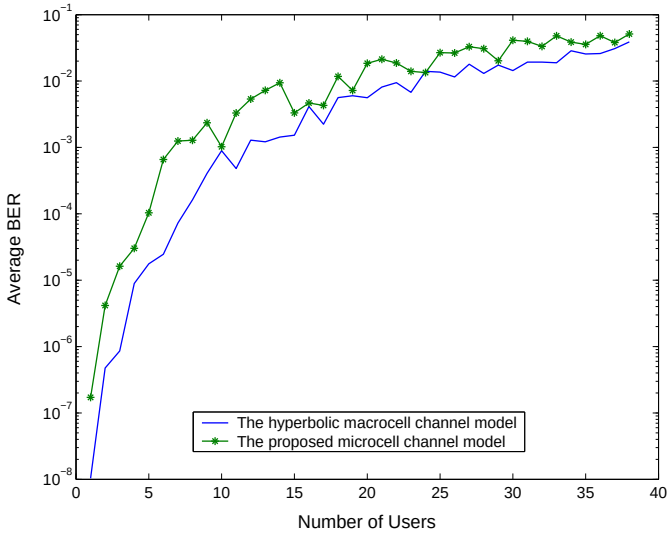

Fig. 11. BER performance comparison between the space-time hyperbolic channel model and the exponential model: the process gain is N= 32, the number of paths is L_m = 20, and the chip rate is 8 Mb/s.

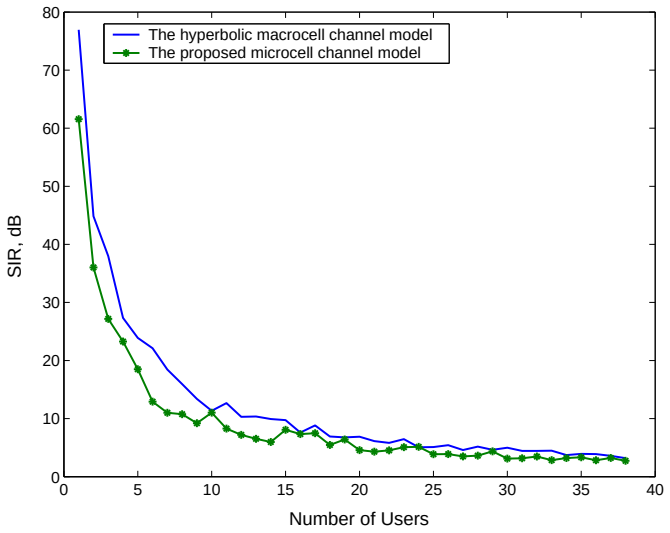

Fig. 12. SIR performance comparison between the space-time hyperbolic channel model and the exponential model: the process gain is N= 32, the number of paths is L_m = 20, and the chip rate is 8 Mb/s.

The mobile station is located at the origin of the scatterers' circle and the base station is within the circle. This model provides the power of each path, the TOA, and the DOA of the multipath component. The joint pdf of the power-DOA and the power-Doppler frequency shift for the proposed channel model are derived and simulated. Simulation results showed that the joint power-Doppler frequency pdf is highly dependent on θ_v.

The simplified expression for the improved Gaussian approximation (SEIGA) in case of imperfect power control for wideband channel model has been used to evaluate the BER and the SIR. As expected, the DS-CDMA cellular sys-

tem performs better in a free space and indoor as compared with other scenarios (like urban and shadowed urban). It is also shown that the performance of the DS-CDMA cellular system is different in the microcell channel model from that in the macrocell model.

ACKNOWLEDGEMENT

The authors would like to thank Prof. R. Janaswamy from the Department of Electrical and Computer Engineering, Naval Postgraduate School, Monterey, CA, USA, and Dr. Q. H. Spencer, from the Distribution Control Systems, Inc., Hazelwood, Missouri, USA for their help in providing the practical measurement data that is used to validate the model.

Appendix

To determine the joint pdf $f(\theta, \psi)$, a transformation of the random variable (r, ψ) into the random variable (θ, ψ) is performed by

$$f(\theta, \psi) = |J(r, \psi)|\, f(r, \psi)\Big|_{r=\frac{D\tan(\theta)}{\sin(\psi)+\cos(\psi)\tan(\theta)}} \tag{60}$$

where r is the distance between MS and scatterer, and $J(r, \psi)$ is the Jacobian of the transformation and we restrict it to be positive. From Fig.1 we get

$$r = \frac{D\tan(\theta)}{\sin(\psi) + \cos(\psi)\tan(\theta)}. \tag{61}$$

The Jacobian $J(r, \psi)$ is given by

$$J(r, \psi) = \left| \frac{\partial r}{\partial \theta} \right| = \frac{D\sin(\psi)\sec^2(\theta)}{(\sin(\psi) + \cos(\psi)\tan(\theta))^2} \tag{62}$$

By substituting (17), (61) and (62) into (60) we get

$$f(\theta, \psi) = \frac{g(\theta, \psi)}{2\pi \tanh(aR)\cosh^2(a\, h(\theta, \psi))} \tag{63}$$

where

$$h(\theta, \psi) = \frac{D\tan(\theta)}{\sin(\psi) + \cos(\psi)\tan(\theta)} \tag{64}$$

and

$$g(\theta, \psi) = \frac{a\ D\sin(\psi)\sec^2(\theta)}{(\sin(\psi) + \cos(\psi)\tan(\theta))^2}. \tag{65}$$

References

[1] A. F. Naguib, *Adaptive Antenna for CDMA Wireless Networks*, *Ph.D. thesis*, Stanford University, USA,, Aug. 1996.

[2] H. Meyr, M. Moeneclaey, and S. A. Fechtel, *Digital Communication Receivers-Synchronisation, Channel Estimation and SignalProcessing*, Wiley Series in Telecommunications and Signal Processing, John Wiley and Sons, Inc., 1998.

[3] M. Stege, J. Jelitto, M. Bronzel, and G. Fettweis, "A Space-Time Channel Model with Stochastic Fading Simulation," *ITG-Fachtagung Intelligente Antennen*, Stuttgart, Germany, pp.1-6, Apr. 1999.

[4] J. M. Holtzman, "A simple, accurate method to calculate spread-spectrum multiple-access error probabilities," *IEEE Transactions on Communications*, vol. 40, no. 3, pp. 461-464, March 1992.

[5] J. C. Liberti and T. S. Rappaport, "A geometrically based model for line-of-sight multipath radio channels," *Proc. of the IEEE Veh. Tech. Conf.*, pp. 844-848, Apr. 1996.

[6] Seedahmed S. Mahmoud, Zahir M. Hussain, and Peter O'Shea, "Space-time model for mobile radio channel with hyperbolically distributed scatterers," *IEEE Antennas and Wireless Propagation Letters*, vol. 1, no. 12, pp. 211-214, 2002.

[7] ———, "Geometrical model for mobile radio channel with hyperbolically distributed scatterers," *The 8th IEEE International Conference on Communications Systems*, vol. 1, pp. 17-20, Singapore, Nov. 2002.

[8] ———, "Properties of the Hyperbolic Macrocell Channel Model: Path Power and Doppler Shift Statistics," *2003 Australian Telecommunications Networks and Applications Conference*, (*ATNAC*), Australia, Dec. 2003.

[9] J. C. Liberti, and T. S. Rappaport, "Accurate techniques to evaluate CDMA bit error rates in multipath channels with imperfect power control," *Communications Theory Mini-Conference, Globecom'95, Singapore*, pp. 33-37, Nov. 1995.

[10] P. Petrus, J. H. Reed, and T. S. Rappaport, "Geometrical-based statistical macrocell channel model for mobile environments," *IEEE Transactions on Communications*, vol. 50, pp. 495-502, March 2002.

[11] T. S. Rappaport, *Wireless Communication- Principles and Practice*, Prentice-Hall, 1996.

[12] R. B. Ertel, and J. H. Reed, "Impact of path-loss on the Doppler spectrum for the geometrically based single bounce vector channel models," *IEEE Veh. Tech. Conf.*, pp. 586-590, 1998.

[13] Q. H. Spencer, B. D. Jeffs, M. A. Jensen, and A. L. Swindlehurst, "Modeling the Statistical Time and Angle of Arrival Characteristics of an Indoor Multipath Channel," *IEEE Journal on Selected Areas in Communications*, vol. 18, NO. 3, pp. 347-360, Mar. 2000.

[14] R. Janaswamy, "Angle and Time of Arrival Statistics for the Gaussian Scatter Density Model," *IEEE Transactions on Wireless Communications*, vol. 1, No. 3, pp. 488-497, July 2002.

[15] J. S. Lehnert, and M. B. Pursley, "Error probabilities for binary direct-sequence spread-spectrum communications with random signature sequences," *IEEE Transactions on Communications*, vol.COM-35, no. 1, pp. 87-98, Jan. 1987.

[16] M. O. Sunay, and P. J. McLane, "Calculating error probabilities for DS-CDMA systems: When not to use the Gaussian approximation," *IEEE Global Telecommunications Conference, Globecom'96*, vol. 3, pp. 1744-1749, Nov. 1996.

[17] J. Mar, and H. Y. Chen, "Performance analysis of cellular CDMA networks over frequency-selective fading channel," *IEEE Transactions on Vehicular Technology*, vol. 47, no. 4, pp. 1234 -1244, Nov. 1998.

[18] G. R. Cooper, and C. D. McGillem, *Probabilistic Methods of Signal and System Analysis*, Holt, Rinehart and Windston, New York, 1986.